

# Nano-crystal formation of Mg-Cu-Gd amorphous ribbon deformed by forced cold rolling

J S Park<sup>1\*</sup>, E S Park<sup>2</sup>

<sup>1</sup> Associate Professor, Department of Materials Science & Engineering, Hanbat National University, Daejeon 305-719, Republic of Korea

<sup>2</sup> Associate Professor, Research Institute for Advanced Materials, Department of Materials Science & Engineering, Seoul National University, Seoul 151-742, Republic of Korea

\*E-mail: [jsphb@hanbat.ac.kr](mailto:jsphb@hanbat.ac.kr)

**Abstract.** Structural and devitrification behaviors of selected Mg-based amorphous alloys have been investigated for the Mg-Cu-Gd amorphous ribbon fabricated by repeated forced cold rolling. When amorphous ribbons were cold-rolled up to a thickness ratio of ~ 50%, the heat of crystallization ( $\Delta H_x$ ) exhibited a reduction. In order to identify devitrification manner of the amorphous alloys, in-situ TEM (Transmission Electron Microscope) observations up to 623 K have been carried out for the as-fabricated ribbon and cold-rolled ribbon at 10 K temperature interval from 423 K. The nano-crystallization behaviors and mechanism of Mg-Cu-Gd alloy ribbon are discussed in terms of TEM observations and kinetic analysis.

## 1. Introduction

The large size bulk metallic glasses (BMGs) have received attention due to their unique properties and controllable crystallization behaviors [1]. Recent investigations have shown that partially devitrified amorphous materials with fine nanocrystals embedded in the amorphous matrix often exhibit controllable microstructures and mechanical properties, and structural stability of amorphous materials has been investigated via deformation-induced process [2-6]. It appears that the devitrification process of amorphous phases via heat treatments is relatively well understood. However, the deformation-induced crystallization phenomena are not fully understood for some examined systems [4,7,8].

Among the reported systems, deformation induced crystallization of Al-based amorphous alloys has been relatively well defined in severe deformation environments such as tensile / compressive tests or rolling process [8,9]. For example, the presence of quenched-in-nuclei in an amorphous state can play a significant role for crystallization in a severe deformation environment [9]. However, other amorphous systems such as Zr-, Cu-, Fe- or Mg-based systems often show different responses for applied extents of deformation [3,6,8,10,11]. For example, the previously reported amorphous systems did not exhibit a consistent devitrification process after cold-rolling [3,8,10,11,12], implying that the applied deformation on amorphous alloys does not necessarily exhibit a similar crystallization behaviour at room temperature. Again, when amorphous ribbon specimens were cold-rolled, the trends of the DSC peak shift were not consistent upon the composition of amorphous ribbons at the similar amount of deformation [8, 12], suggesting that the devitrification behaviour may be dependent on the atomic scale homogeneity of BMGs [13,14,15]. In this regard, it is useful to scrutinize the devitrification behaviour by cold rolling of a form of amorphous ribbons with variable systems, since the amorphous phase can be obtained as the form of ribbon by a relatively well established route. At the same time, as aforementioned, even though several interesting features of BMG systems have been reported, the underlying mechanism during deformation induced crystallization has not been widely investigated for BMG systems. For example, the devitrification behaviors of Mg amorphous alloys are not systematically investigated, when a severe deformation is applied [12]. Thus, it is worthwhile to scrutinize deformation responses for amorphous materials in order to study the structural instability



during severe deformation, and it is of fundamental interest to examine if Mg amorphous material does follow a regular devitrification behavior after severe deformation.

In this study, the Mg-Cu-Gd materials systems with reported compositions [16-19] have been selected in order to provide a guideline for understanding the crystallization reactions by cold rolling and to give a clue for controlling factors during severe deformation. The selected amorphous ribbons were cold-rolled, and microstructural evolution of the amorphous ribbons was investigated with a TEM (Transmission Electron Microscope, JEOL 300KVJEM-3011) equipped with heating facilities.

## 2. Experimental procedure

The Mg alloy ingot was fabricated under an Ar atmosphere in a high frequency furnace. The fabrication process for magnesium ingots is well described in previous reports [16]. The amorphous ribbon was produced by melt spinning process with a surface wheel speed of 40 m/sec. In order to examine the structural and devitrification effect of severe deformation, the amorphous ribbons were cold-rolled by a twin roll. The rolling process was performed by electric motor-controlled twin roll with a diameter of 20 cm at a constant speed of 2.0 radians/sec. Since the cross section of the amorphous ribbon does not critically show the difference except thickness variations, the surface outlook of the cold rolled ribbon (before and after rolling) was observed after cold rolling (**Fig. 1**). A single amorphous ribbon sandwiched by two clean stainless steel plates was repeatedly cold rolled. The thicknesses of the amorphous ribbons were measured by every single path. After rolling, the specimen was elongated towards the rolling directions. The cold rolled specimen was carefully collected, and thermal analyses have been carried out. The microstructures of the amorphous alloys were examined by TEM (Transmission Electron Microscope, JEOL 300KVJEM-3011) with increasing temperature up to ~623 K with a 10 K interval. The thermal history of the cold-rolled specimens was investigated by DSC (Differential Scanning Calorimetry (Perkin Elmers DSC-7)) with a various heating rate.



Fig. 1 specimen outlook before and after cold rolling indicating that the ribbon is elongated after the rolling [12]

### 3. Results and Discussion

Fig. 2 shows DSC curves of the  $Mg_{85}Cu_5Gd_{10}$  amorphous ribbon which exhibit a glass forming ability (GFA) of less than 1 mm [16]. In order to identify the devitrification behaviours after different amounts of cold rolling, the piece of specimen was collected after 35% of thickness reduction. When the  $Mg_{85}Cu_5Gd_{10}$  alloy was cold rolled, the DSC curves show a difference between as-spun ribbon and cold rolled ribbon. Fig. 3 is the enlargement of the marked area in Fig. 2. It shows that when the ribbon was cold rolled, there is a difference in  $\Delta H$ (relaxation) compared with as-spun ribbon, suggesting that the forced deformation of the amorphous alloy exhibits nanoscale aggregation. In order to clarify the difference between as-spun ribbon and cold-rolled ribbon, the glass transition temperature ( $T_g$ ), crystallization temperature ( $T_x$ ) and peak temperature with respect to the heating rate ( $T_p$ ) were enlisted in Table 1 and Table 2.

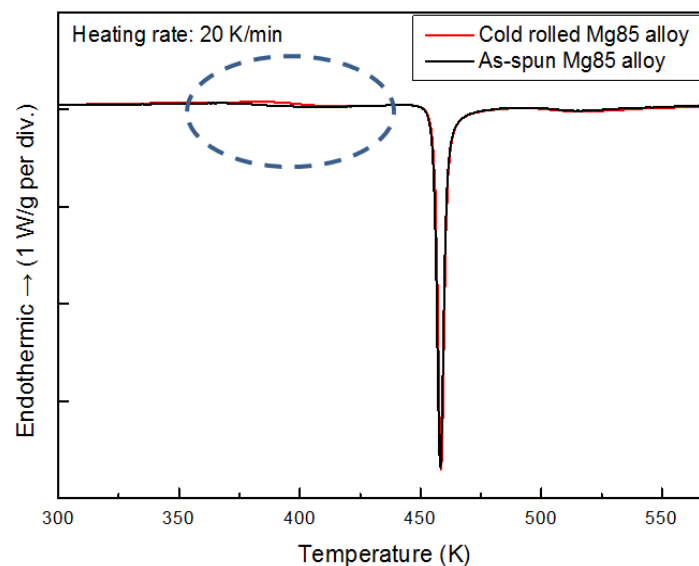


Fig. 2 Continuous heating DSC curves of the  $Mg_{85}Cu_5Cd_{10}$  amorphous alloy with a heating rate of 20 K/min (a) as-spun ribbon with a thickness of 45  $\mu\text{m}$  (b) cold-rolled ribbon with a thickness reduced from 45 to 27  $\mu\text{m}$

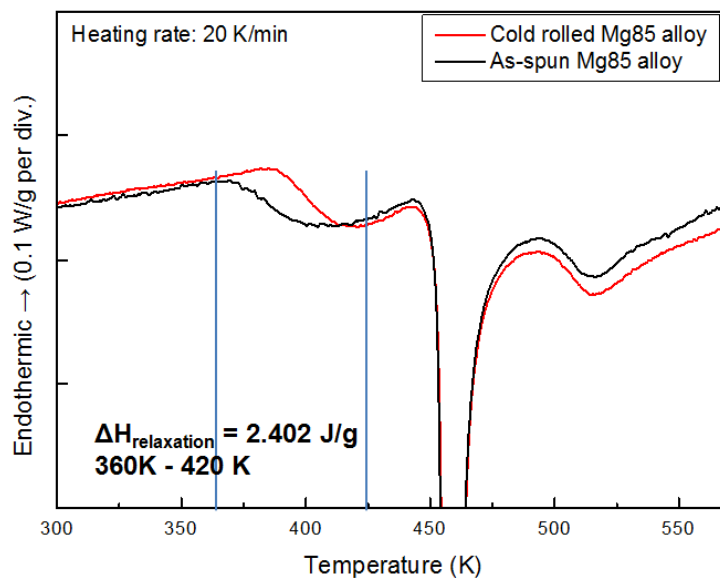


Fig. 3 Continuous heating DSC curves of the  $Mg_{85}Cu_5Cd_{10}$  amorphous alloy with a heating rate of 20 K/min (The enlargement of the marked area in Fig. 2).

Table 1 and Table 2 show that  $\Delta H$  is reduced with increasing heating rate, as expected. At the same time,  $\Delta H$  is reduced for the cold rolled ribbon compared with as-spun ribbon, indicating that the specimen undergoes nanoscale agglomeration or atomic scale bias. In order to identify the structural evolution with heating, TEM observations have been carried out with an interval of 10 K up to 623 K.

Table 1  $T_g$ ,  $T_x$  and  $T_p$  of as-spun ribbon with respect to the heating rate

Heating rate	$T_g$ (K)	$T_x$ (K)	$T_p$ (K)	$\Delta H$ (J/g)
5 K/min	416.25	447.46	449.46	-48.5335
10 K/min	420.59	451.51	453.8	-50.4691
20 K/min	429.38	455.37	458.17	-49.0793
40 K/min	438.92	459.89	463.45	-51.5000
80 K/min	446.75	466.14	471.05	-52.2751

Table 2  $T_g$ ,  $T_x$  and  $T_p$  of cold rolled ribbon with respect to the heating rate

Heating rate	$T_g$ (K)	$T_x$ (K)	$T_p$ (K)	$\Delta H$ (J/g)
5 K/min	424.13	447.70	449.69	-46.3941
10 K/min	427.12	451.63	454.05	-47.5700
20 K/min	432.96	455.84	458.42	-47.0728
40 K/min	439.30	460.69	463.75	-47.9769
80 K/min	447.60	466.05	470.51	-50.4435

Fig. 4 shows TEM of the as-spun ribbon (a) at room temperature and (b) heated up to 433 K. TEM shows that the as-spun ribbon does not crystallize at room temperature as shown in Fig. 4 (a). However, when the specimen was heated up to 433K, the specimen started to crystallize as shown in Fig. 4 (b). While crystallization part was not clearly identified, some part was noted as crystallization evidence as shown in Fig. 4(b). Fig. 5 shows the as-cold rolled ribbon at room temperature (Fig. 5(a)) and the cold rolled ribbon heated up to 483 K (Fig. 5 (b)). When the ribbon was cold rolled, a partial crystallization has been estimated as shown in Table 1. However, the clear crystallization figures were not clearly observed. A detailed discussions will be reported elsewhere. In the other hands, when the cold-rolled specimen was heated, a crystallization was clearly observed. It is noteworthy that the crystallization temperature of the cold rolled specimen was different from that of the as-spun ribbon. When the as-spun ribbon was heated, the crystallization temperature was observed as  $\sim 433\text{K}$ . However, for the cold rolled specimen, the crystallization temperature was observed as  $\sim 483\text{K}$ . Thus, it appears that the resistance for crystallization for cold rolled specimen was increased, compared with as-spun ribbon.

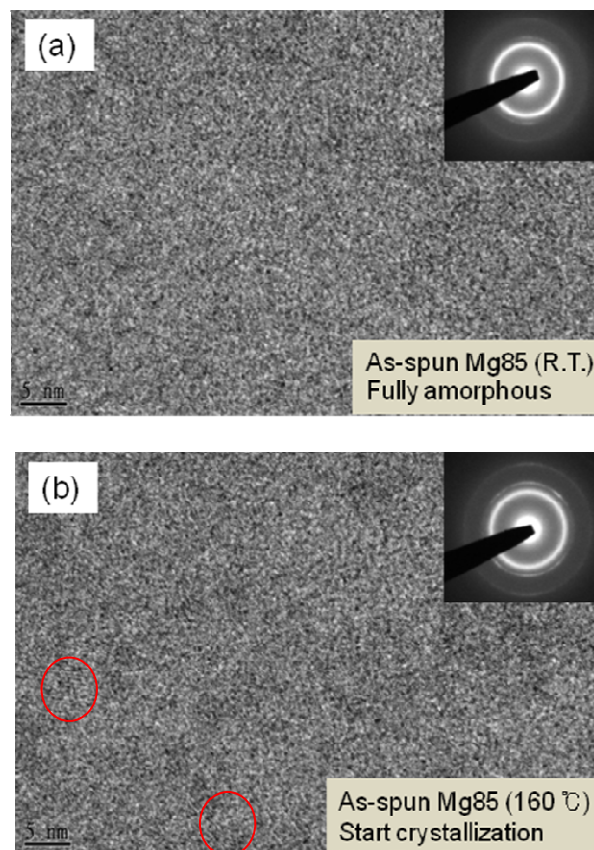


Fig. 4 TEM of (a) as-spun ribbon at room temperature and (b) heated ribbon up to 433 K

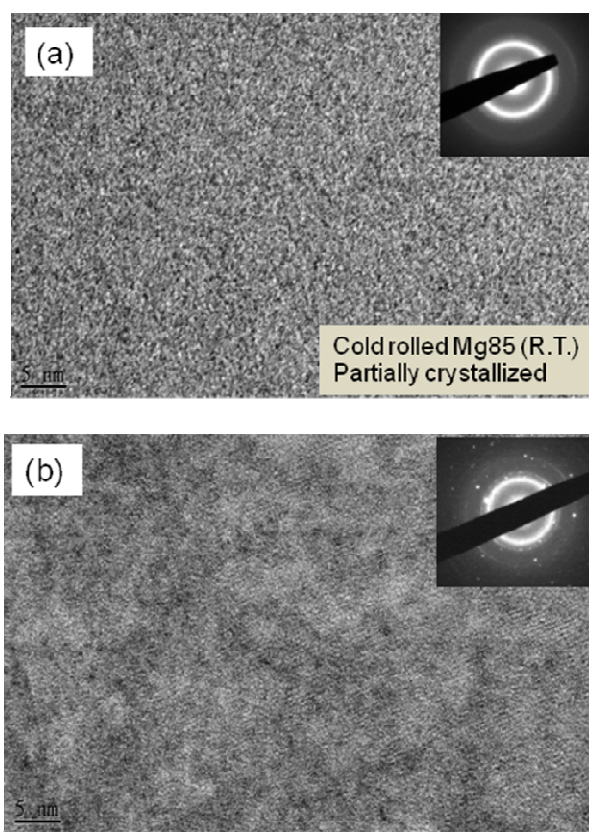


Fig. 5 TEM of (a) as- cold rolled ribbon at room temperature and (b) heated cold rolled ribbon up to 483 K

Regarding the deformation induced devitrification, when  $\text{Cu}_{46}\text{Zr}_{47}\text{Al}_7$  amorphous alloy was severely cold rolled, the  $\Delta H_x$  was not clearly affected, even though the thickness was significantly reduced. The deformation-induced nano-crystalline phase formation has been previously reported in Al-based amorphous alloys, and was attributed to the adiabatic heating near shear bands during applied loading. The shear band formation induces a dilatation of free volume inside the shear bands, leading to nanocrystallization by the thermal diffusion resulting from temperature rise [17,18]. In contrast, it has also been suggested that since the atomic density of the shear band area is lower than that of the surrounding matrix, the applied stress can lead to the enhancement of atomic diffusional mobility within the shear bands, and that the high atomic mobility during deformation results in local reordering during the shear band formation [4].

At the present observations, the partial devitrification of the  $\text{Mg}_{85}\text{Cu}_5\text{Gd}_{10}$  alloy with GFA of less than 1 mm was observed after cold rolling. It is interesting that the severe deformation of the amorphous alloys with low GFA can enhance the atomic mobility. On the other hand, the current observations clearly show that the initial devitrification induced by severe deformation does not critically affect the extents of resistance for crystallization. When the temperature of specimens was increased, the severely cold rolled amorphous Mg ribbon retards crystallization temperature ( $\sim 483\text{K}$ ), compared with as-received ribbon ( $\sim 433\text{K}$ ). This indicates that the amorphous matrix does undergo relaxation which may stabilize the matrix. Thus, the cold rolled specimen increases the resistance for crystallization as shown in Fig. 4 and Fig. 5, which is against the previous observations that the atomic-scaled homogeneity is generally modified by cold rolling and crystallization reactions are enhanced due to the possible atomic scale intermixing [4,7].

While further investigations are needed for identification of crystallization behaviors of other Mg amorphous alloys, the current observations suggest that the severe deformation of Mg amorphous alloys increases the resistance for crystallization during heating, which indicates that the crystallization pathway of Mg amorphous alloys can be biased depending on the applied deformation resulting from atomic movements.

#### 4. Summary

Structural and devitrification behaviors of selected Mg<sub>85</sub>Cu<sub>5</sub>Gd<sub>10</sub> amorphous alloys have been investigated in order to identify the effect of forced cold rolling on the amorphous ribbon. When the amorphous ribbons were cold rolled,  $\Delta H_x$  (recovery) exhibited a modification after the rolling. In order to identify devitrification manner of the amorphous alloys, in-situ TEM (Transmission Electron Microscopy) observations up to 623 K have been carried out for the as-fabricated ribbon and cold-rolled ribbon at 10 K temperature interval from 423 K. When the cold rolled and as-spun ribbon specimen was observed with in-situ TEM, the severely cold rolled amorphous Mg ribbon shows crystallization temperature of ~ 483K, but the as-spun ribbon does that of ~433 K. The TEM observations show that the relaxation of the Mg matrix is affected by cold rolling stabilizes the matrix. Thus, it appears that the resistance for crystallization is increased for the cold rolled specimen during heating stage.

#### Acknowledgments

One of the authors (E.S. Park) was supported by the Center for Iron and Steel Research at Research Institute of Advanced Materials (RIAM) and Engineering Research Institute at Seoul National University.

#### References

- [1] Kim DH, Kim WT, Park ES, Mattern N and Eckert J 2013 Prog. Mater. Sci. **58** 1103
- [2] Louzguine DV and Inoue A 2004 Mater. Sci. Eng. A **375-377** 346
- [3] Jiang WH, Pinkerton FE, Atzmon M 2005 Acta Mater. **53** 3469
- [4] Perepezko JH, Kimme KE and Hebert RJ, 2009 J. alloys compd. **483** 14
- [5] Tian JW, Shaw LL, Wang YD, Yokoyama Y and Liaw PK 2009 Intermetallics **17** 951
- [6] Park JS, Lim HK, Kim JH, Chang HJ, Kim WT, Kim DH and Fluery E, 2005 J. Non. Cryst. Solids **351** 2142
- [7] Schuh CA, Hufnagel TC, Ramamurty U 2007 Acta Mater. **5** 4067
- [8] Jin HJ, Zhou F, Wang LB and Lu K 2001 Scr. Mater. **44** 1083
- [9] Hebert RJ, Perepezko JH, Rosner H, Wilde G 2006 Scr. Mater. **54** 25
- [10] Yokoyama Y, Yamano K, Fukaura K, Sunada H and Inoue A 2001 Mater. Trans. , JIM, **42** 623
- [11] Cao QP, Li JF, Zhou YH and Jiang JZ 2008 Scr. Mater. **59** 673
- [12] Park JS, Kim JM and Park ES 2010 Intermetallics **18** 1920
- [13] Lee BJ, Lee CS and Lee JC 2003 Acta Mater. **51** 6233
- [14] Park ES, Kyeong JS, Kim DH 2007 Scr. Mater. **57** 49
- [15] Park ES and Kim DH 2010 Intermetallics **18** 1867
- [16] Men H, Kim DH, 2003 J. Mater. Res. **18** 1502.
- [17] Guo F, Poon SJ, Shiflet GJ 2000 Scr. Mater. **43** 1089
- [18] Inoue A, Ohtera K, Tsai AP and Masumoto T 1988 Jpn. J. Appl. Phys. **27** L479
- [19] Inoue A and Zhang W, 2002 Mater. Trans. **43** 2921